Relationship between Supersaturation Ratio and Supply Rate of Solute in the Growth Process of Monodisperse Colloidal Particles and Application to AgBr Systems

Fumiyuki Shiba* and Yusuke Okawa

Graduate School of Science and Technology, Chiba University, Yayoicho 1-33, Inageku, Chiba 263-8522, Japan

Received: July 8, 2005; In Final Form: September 12, 2005

Supersaturation ratio, S, has been theoretically related to the supply rate of solute, Q, from growth rate and mass-balance equations in the quasi-steady state in the growth process of isotropic monodisperse particles. The derived equation, $(S - 1) = (1/D + 1/kr)(Q/\beta C_0 nr) + 2V_m\gamma/rRT$, suggests a linear dependence of S on Q under constant n and r, where D is the diffusion coefficient, k is the rate constant for surface-reaction, C_0 is the solubility, n and r are the number and radius of growing particles, respectively, V_m is the molar volume of particles, R is the gas constant, T is the absolute temperature, and β is the shape factor defined by $\beta \equiv (1/r^2)\, \mathrm{d}v/\mathrm{d}r$, where v is the volume of an individual particle. The equation was applied to the analysis of growth kinetics and determinations of critical supersaturation ratio in monodisperse AgBr particles in the controlled double-jet system with the assistance of a potentiometric supersaturation measurement. In both cubic and octahedral particles, growth rates were completely limited by diffusion and surface-reaction at pBr ($\equiv -\log[\mathrm{Br}^-]$) 3.0 and 1.0, respectively, while the growths were intermediate of them at pBr 2.0 and 4.0. The growth parameters, DC_0 and kC_0, were experimentally determined. Also, critical supersaturation ratio was estimated as 1.28 as an average in the present study.

Introduction

Monodisperse particles[1,2] are expected as functional materials having sharp distributions of properties. Silver halides prepared by the controlled double-jet (CDJ) technique[3] in the photographic industry may be the most typical utilization of them. In addition, monodisperse particles are important particulate systems in fundamental studies in colloid science. Although relatively low productivity in monodisperse systems has tended to retard scientific and industrial applications, recent progresses are conquering the limitations.

There are two requirements to form monodisperse particles in general.[1,2] Electrostatic repulsion force and protective colloids are common ways to *prevent random coagulations among growing particles*. The "gel-sol method", proposed by Sugimoto,[4−6] also uses a gel-network of precursor, which is eventually consumed by particle growth. Another requirement, *separation of nucleation and growth periods*, is achieved by controlling supersaturation ratio, as expressed in the LaMer diagram.[7] When the supersaturation ratio, S, exceeds the critical one, S^*, spontaneous nucleation will occur. Therefore, S must be kept under S^* after the end of the nucleation period. In addition, $S > 1$ is necessary to avoid broadening of the size distribution by Ostwald ripening. However, actual control of supersaturation is rather complicated, since it involves various factors such as controlling chemical reactions, formation environments, and reservation of resources. Moreover, nanosized monodisperse particles require more sophisticated methods of preparation. Thus, a precise understanding of the formation process is desired. Monodisperse silver halide particles have been frequently employed for this purpose in CDJ,[8−18] spontaneous nucleation,[19,20] and reversed micelle[21,22] systems, due to a wealth of physicochemical data, opportune rates of nucleation and growth, and importance in the photographic industry.

Meanwhile, knowing a determinant of S is important to obtain high formation efficiency without unwanted nucleation during the growth period, since both nucleation and growth rates are functions of S. In the quasi-steady state of growth, all the supplied solutes are immediately consumed by the growth of the particle. This means the molar growth rate of an individual particle equals the molar supply rate of solute per particle. On the other hand, the growth rate is also expressed as a function of S. As the requirements must be satisfied at the same time, controlling Q has practical importance in growth of monodisperse particles, as well as in nucleation processes.[12,17,19,21]

Previously, we formulated S as a function of Q in a complete diffusion-limited growth and applied it to the determination of S^* in monodisperse AgCl systems.[23] However, a more general equation was still desired to adapt to various monodisperse systems. In this study, both diffusion and surface-reaction processes are introduced in the derivation of the relationship between S and Q. By using an in-situ measurement of supersaturation ratio, the equation was validated by monodisperse AgBr systems, in which the growth limiting step can be altered by pBr ($\equiv -\log[\mathrm{Br}^-]$).[24] Growth kinetics and S^* in the cubic and octahedral systems were also evaluated.

Theory

Growth of colloidal particles consists of diffusion and surface-reaction processes. Solutes, or reaction resources, are transported to surfaces of particles from bulk liquid phase by diffusion. Then the solutes are incorporated into the solid by the subsequent surface-reaction. Assuming an infinite thickness of the diffusion layer, these steps can be expressed in terms of the increase

* To whom correspondence should be addressed. E-mail: shiba@faculty.chiba-u.jp.

10.1021/jp053742t CCC: $30.25
Published on Web 10/20/2005

rate of the radius, dr/dt, as

$$\frac{dr}{dt} = \frac{DV_m}{r}(C - C_i) \quad (1)$$

and

$$\frac{dr}{dt} = kV_m(C_i - C_r) \quad (2)$$

for the diffusion and reaction steps, respectively, where r is the radius of an inscribed sphere of isotropic polyhedral particles, t is the time, D is the diffusion coefficient, k is the rate constant of the surface-reaction, V_m is the molar volume of particles, and C, C_i, and C_r are the solute concentrations in the bulk liquid phase, at the solid−liquid interface, and in equilibrium with the particle with radius r, respectively. Because the processes are successive, dr/dt in eqs 1 and 2 must be equal. Combining eq 1 with eq 2 to eliminate C_i, one obtains

$$\frac{dr}{dt} = \frac{DkV_mC_0}{D + kr}\left(S - \frac{C_r}{C_0}\right) \quad (3)$$

where S is the supersaturation ratio defined by $S \equiv C/C_0$ and C_0 is the solubility or the equilibrium concentration of the bulk solid. Equation 3 may be translated to a volume increase rate, dv/dt, as

$$\frac{dv}{dt} = \beta r^2\frac{DkV_mC_0}{D + kr}\left(S - 1 - \frac{2V_m\gamma}{rRT}\right) \quad (4)$$

by substituting the Gibbs−Thomson equation,

$$\frac{C_r}{C_0} = \exp\left(\frac{2V_m\gamma}{rRT}\right) \approx 1 + \frac{2V_m\gamma}{rRT} \quad (5)$$

where the approximation holds under $2V_m\gamma/rRT \ll 1$ and β is the shape factor defined by $\beta \equiv (1/r^2)\,dv/dr$, v is the volume of an individual particle, and γ is the specific interfacial energy of the solid−liquid interface. When the shape of a particle is maintained through the growth period, β is constant and equals 4π (=12.56), $12\sqrt{3}$ (=20.79), and 24 for spherical, octahedral, and cubic particles, respectively, for instance.

In the quasi-steady state of growth, in which the supply and consumption rates of solutes are effectively equal, a mass-balance equation can be described as

$$\frac{dv}{dt} = \frac{QV_m}{n} \quad (6)$$

where n is the number of growing particles in the reaction vessel. The dv/dt on the left-hand side of eq 6 should be equal to dv/dt in eq 4. Hence, one obtains a general relationship between S and Q as

$$S - 1 = \left(\frac{1}{D} + \frac{1}{kr}\right)\frac{Q}{\beta C_0 nr} + \frac{2V_m\gamma}{rRT} \quad (7)$$

in the growth process of isotropic monodisperse particles. Equation 7 clearly indicates a linear relationship between S and Q under constant n and r.

If P is defined by the slope of a plot of $(S - 1)$ vs Q/nr, P will be linearly related to r^{-1} as

$$P = \frac{1}{\beta DC_0} + \frac{1}{\beta kC_0}\frac{1}{r} \quad (8)$$

Thus, the growth parameters, DC_0 and kC_0, can be given by the intercept and slope, respectively, from the r^{-1} dependence of P in eq 8. When the growth is completely limited by the surface-reaction ($D \gg kr$), the first term on the right-hand side of eq 8 is negligible and thus P will be proportional to r^{-1}. On the contrary, P will be independent of r in complete diffusion-limited growths ($D \ll kr$), since the second term on the right-hand side of eq 8 is much smaller than the first term in this case. Hence, plotting P compared to the inverse of r reveals the growth limiting step.

When S exceeds S^* in a large Q/nr region, some new nuclei will be formed and the total number of particles in the reaction vessel becomes larger than n. In this case, S will be lowered from the anticipated linear relationship of eq 7. In other words, S at the inflection point in the $(S - 1)$ vs Q/nr plot can be defined as S^*, as discussed in the previous study.[23]

Experimental Section

Preparation of Monodisperse Seed Particles. The CDJ technique was applied to prepare the monodisperse seed particles of cubic and octahedral AgBr ones at pBr 4.0 and 2.0, respectively, in 3.0% gelatin solutions at 50 °C. The particles were centrifuged three times to remove the soluble salts and excess gelatin. Then the particles were redispersed in a 2.0% gelatin solution and stored in a refrigerator as the stock. For each cubic and octahedral system, three kinds of seed dispersions with different sizes were prepared. The mean radii were r = 0.065, 0.12, and 0.22 μm for both shapes from TEM observations. The coefficients of variation in radii (within 5%) were sufficiently low to regard them as monodisperse systems. To determine the silver contents in the stocks, a certain amount of each stock was dissolved in a sodium thiosulfate solution (24%) and then subjected to a potentiometric titration with thioacetamide.[25] The particle number in a unit weight of the stock was then estimated from the silver content and mean radius.

Measurement of S in the Growth Process. The relationship between S and Q/nr in the growth process was evaluated by introducing reactant solutions to a dispersion of the seed particles by the CDJ technique with monitoring of S as follows. The stock was accurately weighed ($n = 1 \times 10^{11}$) and dissolved to disperse the seed particles in a 250 cm^3 of 2.0% gelatin solution in an 1-L Pyrex beaker at 50 °C. Potassium bromide was added to adjust the pBr. With sufficient stirring, $AgNO_3$ and KBr solutions were continuously introduced to the seed dispersion toward the impeller at 50 °C. Here, Ag^+ and Br^- ion-selective electrodes, situated at the periphery in the vessel, were simultaneously used to determine S directly from the potentials[23,26] as $S \equiv [Ag^+][Br^-]/K_{sp}$,[20] where $[Ag^+]$ and $[Br^-]$ are the concentrations of Ag^+ and Br^- ions in the bulk liquid phase, respectively, and K_{sp} is the solubility product of sparingly soluble AgBr. The molar supply rate of $AgNO_3$ solution, Q, was kept constant through each run while that of KBr solution was regulated to keep pBr constant. The dependence of P on r was evaluated with all kinds of seed particles. Values of S^* were determined only in $r = 0.12$ μm.

The concentration of $AgNO_3$ solution was 5.0×10^{-3} mol dm^{-3} in pBr 1.0 but 5.0×10^{-4} mol dm^{-3} in other pBr conditions, while the concentrations of KBr solutions were 0.205, 2.05×10^{-2}, 2.50×10^{-3}, and 7.0×10^{-4} mol dm^{-3} for pBr 1.0, 2.0, 3.0, and 4.0, respectively. Ag_2S-coated and AgBr-coated silver electrodes were used as the Ag^+ and Br^- ion-selective electrodes, respectively. An inert deionized gelatin (P-3201, Nitta Gelatin) was employed in the present study.

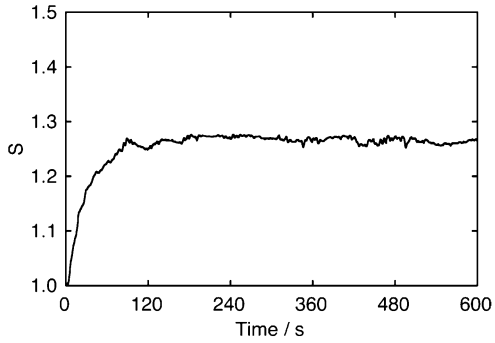

Figure 1. Time evolution curve of supersaturation ratio by introducing the reactants to a seed dispersion of octahedral AgBr particles in pBr 2.0 at 50 °C, where $r = 0.12$ μm and $Q/nr = 2.56 \times 10^{-12}$ mol s^{-1} m^{-1}.

Results and Discussion

Figure 1 is a time evolution curve of supersaturation ratio when introducing the reactants to a seed dispersion (octahedral particles, $r = 0.12$ μm) in pBr 2.0, where $Q/nr = 2.56 \times 10^{-12}$ mol s^{-1} m^{-1}. After a rising period, S reached a plateau, or quasi-steady state. At high regions of Q/nr, on the other hand, maxima in S were observed due to an increase of consumption rates by nuclei newly formed in $S > S^*$. The time at which S attains a plateau or maximum was almost the same (Figure 1) for pBr 2.0, 3.0, and 4.0, but it was at ~30 s in pBr 1.0, because of the about 10-fold higher Q/nr in pBr 1.0 than the other pBr conditions due to the higher solubility and thus faster growth rate. The raising period probably reflects accumulation of solutes as $AgBr_i^{(i-1)-}$ and Ag^+−gelatin complexes, as their concentrations are also functions of S. Hence, the supersaturation ratio at the plateau or maximum was employed as S for the following analyses.

Meanwhile, it has been known that AgBr particles can change their shape to more stable forms by additional growth, depending on the pBr.[28] In the present study, cubic seed particles became octahedral ones after 600 s of growth in pBr 1.0. In other pBr conditions, such transformations were observed only in $r = 0.065$ μm systems, since the amounts of supplied reactants were insufficient for the shape changes of larger seed particles. However, the influence of the shape alteration on the following analyses is negligible, since the S values were determined at an earlier stage of growth compared to the time required for the shape to change by growth. It is thus valid to regard the experimental results for cubic and octahedral particles as those for {100} and {111} faces, respectively.

Figure 2 shows the relationships between $(S - 1)$ and Q/nr for octahedral particles at pBr 2.0. For $r = 0.12$ μm, an inflection point was clearly observed at $Q/nr = 2.70 \times 10^{-12}$ mol s^{-1} m^{-1}, giving $S^* = 1.28$. In accordance with eq 7, $(S - 1)$ was linearly related to Q/nr in the region of $S < S^*$ for each particle size. As shown in Figure 3, the slope, P, was also linearly related to the inverse of r as suggested by eq 8. The existence of a slope and intercept in Figure 3 implies the growth in this condition is "intermediate," in which the contributions of diffusion and reaction processes are comparable. The slope (6.1×10^3 m s mol^{-1}) and intercept (4.0×10^{10} m s mol^{-1}), corresponding to $1/\beta C_0 k$ and $1/\beta C_0 D$, respectively, give $k/D = 6.6 \times 10^6$ m^{-1}. If $C_0 = 6.1 \times 10^{-7}$ mol dm^{-3} is assumed, one obtains $D = 2.0 \times 10^{-5}$ cm^2 s^{-1} and $k = 1.3 \times 10^{-2}$ m s^{-1}, where $\beta = 12\sqrt{3}$ and C_0 is a calculated value of the total concentration of $AgBr_i^{(i-1)-}$ and Ag^+−gelatin complexes including free Ag^+ from the equilibrium constants in the literature.[17]

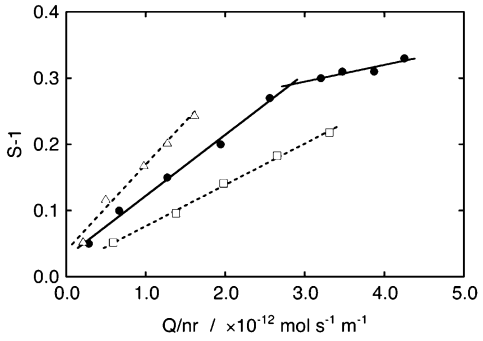

Figure 2. Relationship between $(S - 1)$ and Q/nr for octahedral AgBr particles in pBr 2.0, where $r = 0.065$ μm (△), 0.12 μm (●), and 0.22 μm (□). The inflection point in $r = 0.12$ μm gives $S^* = 1.28$ as the critical supersaturation ratio.

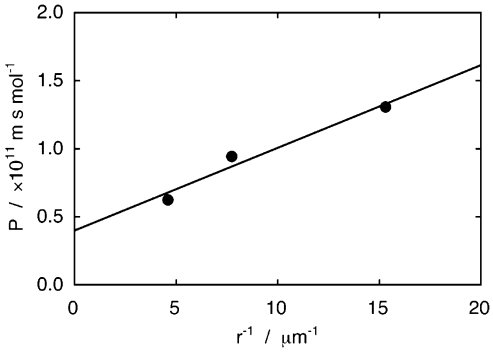

Figure 3. Dependence of P on the inverse of r for octahedral AgBr particles in pBr 2.0, where P values were determined from the slopes in Figure 2 in the region of $S < S^*$.

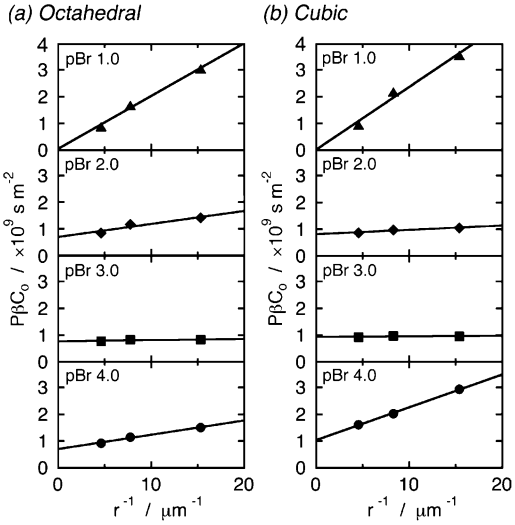

Figure 4. Dependence of $P\beta C_0$ on the inverse of r, where C_0 is assumed as the total concentration of $AgBr_i^{(i-1)-}$ and Ag^+−gelatin complexes including free Ag^+ ions[17] as listed in Table 1: (a) octahedral particles; (b) cubic particles.

Using $P\beta C_0$ instead of P may be preferable in order to compare the behavior of the system as a function of experimental conditions, because of the large difference in C_0 (see Figure 10 in ref 17). In addition, $\beta = 24$ for cubic particles while $\beta = 12\sqrt{3}$ for octahedral ones. Figure 4 is the relationship between $P\beta C_0$ and r^{-1} in the tested conditions, where C_0 is estimated as above and listed in Table 1. It should be noted that, however, so-calculated C_0 is only an assumption for comparison. In both cubic and octahedral particles, $P\beta C_0$ values were proportional to r^{-1} at 1.0 and independent of r^{-1} at pBr 3.0. In other words, the growth rates of both {100} and {111}

TABLE 1: Experimental Results of Growth Parameters Obtained from the Slopes and Intercepts in Figure 4 by Application of Eq 8 and Critical Supersaturation Ratios Estimated from the Inflection Points in the ($S - 1$) vs Q/nr Plots

	pBr 1.0		pBr 2.0		pBr 3.0		pBr 4.0	
	octahedral	cubic	octahedral	cubic	octahedral	cubic	octahedral	cubic
limiting step	reaction	reaction	intermediate	intermediate	diffusion	diffusion	intermediate	intermediate
DC_0 (mol s^{-1} m^{-1})			1.2×10^{-12}	7.9×10^{-13}	2.7×10^{-13}	2.3×10^{-13}	6.3×10^{-13}	4.3×10^{-13}
D (cm^2 s^{-1})			2.0×10^{-5}	1.3×10^{-5}	1.3×10^{-5}	1.1×10^{-5}	1.5×10^{-5}	1.0×10^{-5}
kC_0 (mol s^{-1} m^{-2})	4.5×10^{-5}	3.8×10^{-5}	7.9×10^{-6}	2.2×10^{-5}			8.3×10^{-6}	3.6×10^{-6}
k (m s^{-1})	4.9×10^{-3}	4.2×10^{-3}	1.3×10^{-2}	3.7×10^{-2}			1.9×10^{-2}	8.4×10^{-3}
k/D (m^{-1})	0	0	6.6×10^{6}	2.8×10^{7}	∞	∞	1.3×10^{7}	$8. \times 10^{6}$
k_{111}/k_{100}	1.18		0.35				2.31	
S^*	1.29	1.27	1.28	1.30	1.21	1.26	1.30	1.33
C_0[a] (mol dm^{-3})	9.1×10^{-6}		6.1×10^{-7}		2.1×10^{-7}		4.3×10^{-7}	

[a] Calculated from equilibrium constants for $AgBr_i^{(i-1)-}$ ($i = 0-4$) and Ag^+−gelatin conplexes.[17]

faces of AgBr are completely limited by surface-reaction at pBr 1.0 and by diffusion at pBr 3.0. Growths in pBr 2.0 and pBr 4.0 seem intermediate between them. The results obtained from Figure 4 are summarized in Table 1, where DC_0, or D, was not obtained in pBr 1.0, since the first term in eq 8 equals zero. Likewise, kC_0, or k, in pBr 3.0 was not determined.

Unfortunately, the present study does not provide the explanations for the pBr dependence of the growth limiting step experimentally. However, adsorption of Br^- ions on particle surfaces is a possible reason for the pBr dependence of k. That is, if adsorbed Br^- ions act as a kind of two-dimensional nuclei on a surface, an increase of adsorption raises the rate constant of surface reaction until a certain coverage level. On the other hand, high coverage of adsorbed Br^- ions may retard incorporation of the constituent ions in a crystal lattice. Anyway, more suitable experiments should be conducted to reveal the interesting results.

All of the D values listed in Table 1 are in a reasonable range expected for small species in water medium.[9,11] Since C_0 and D are irrelevant to particle shape, the difference in D in Table 1 reflects the possible experimental errors. On the other hand, the value of k has a meaningful difference. It has been known that the shape of AgBr particles prepared in the CDJ system depends on the pBr condition. Cubic particles bound by six {100} faces, tetradecahedral particles consisting of six {100} and eight {111} faces, and octahedral particles with eight {111} faces are formed in the regions of pBr > 3.5, 3.5 > pBr > 2.5, and 2.5 > pBr, respectively, in the absence of specific growth modifiers such as NH_3.[24,27] As discussed by Sugimoto,[24,28] the ratio of rate constants, k_{111}/k_{100}, determines the shape of AgBr in the growth form in reaction limited conditions, where k_{111} and k_{100} are the rate constants for {111} and {100} faces, respectively. Namely, $k_{111}/k_{100} \geq \sqrt{3}$ yields cubic particles while $k_{111}/k_{100} \leq 1/\sqrt{3}$ gives octahedral ones. The present results at pBr 4.0 and 2.0 satisfy the requirements to produce cubic and octahedral particles, respectively, although they were in incomplete reaction limited growths.

On the contrary, k_{111} and k_{100} were almost the same in pBr 1.0, despite the shape change from cube to octahedron as mentioned above. This contradiction may be explained in terms of equilibrium form,[28] in which the particle shape is determined by the ratio of interfacial energies of particle faces. Although the consequence is not clear, it is interesting that pBr 1.0 is in a region where tabular AgBr particles with parallel twins will be formed.

In general, solubility, C_0, is one of the important factors in both nucleation and growth processes of fine particles. Although C_0 was assumed as the total concentration of $AgBr_i^{(i-1)-}$ and Ag^+ complexes calculated from equilibrium constants in this study, it has not been sufficiently certified as the effective solubility, or activity, in the formation processes of monodisperse particles. Since D listed in Table 1 seems in a reasonable range, the estimation of C_0 probably does not stray so much. However, C_0 and D with such uncertainties give some ambiguities in precise analyses. The experimental determination of DC_0 and kC_0 will provide detailed understandings of the formation processes.

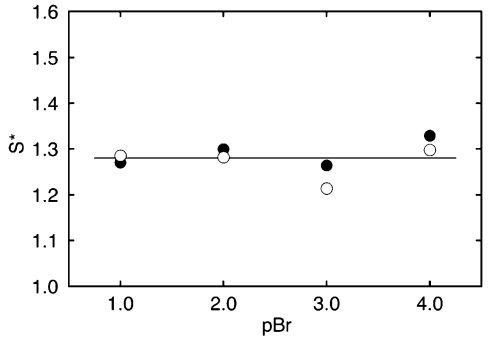

Figure 5. Relationship between S^* and pBr obtained in the octahedral (○) and cubic (●) systems.

The critical supersaturation ratio for AgBr, $S^* = 1.2-1.6$, indirectly estimated in the CDJ system, has been reported from growth rate analysis[9] and TEM observations of nuclei with the Gibbs−Thomson equation.[15] On the contrary, much higher S^* values were reported in closed spontaneous nucleation systems. For example, Sugimoto and Shiba[20] obtained $S_{max} = 3.4-3.8$, regarded as S^*, by using a silver ion-selective electrode. It has been ascribed that the difference in S^* is caused by a peculiar process of formation and consumption of embryos and that r^* is corresponding to the maximum radius of the embryo, r_e^{max}, in the CDJ system.[15,19,20] The present results for S^* with the direct S measurement strongly support the validities of the S^* values in the CDJ system in addition to the physicochemical meanings.

In this study, no clear dependence of S^* on pBr was found, as shown in Figure 5, suggesting r^*, or r_e^{max}, was almost constant. This independence may be endorsed by the recent report by Nakatsugawa and Tani.[29] They observed that the silver potential around addition jets was independent of the bulk pBr in their CDJ system, implying the formation environment of an embryo is also almost independent of pBr in the bulk phase. In the present study, $r^* = 12$ nm is estimated from $S^* = 1.28$ as the average with the Gibbs−Thomson equation and $\gamma = 142$ mJ m^{-2} as a theoretical value for spherical AgBr.[30] Jagannathan and Wey[15] reported 4.2−5.0 nm as an average radius at S_{max} from TEM observations. If a symmetric size distribution is assumed, $r_e^{max} = 8.4-10$ nm is expected. Sugimoto[17] also estimated $r_e^{max} = 8.2$ nm on the basis of a derived equation (eq 46 in ref 17) with application of experimental results. Taking

into account the differences in experimental conditions and CDJ apparatus, r^* in the present study is fairly close to the reported values.

References and Notes

(1) Sugimoto, T. *Monodispersed Particles*; Elsevier: Amsterdam, 2001.
(2) Sugimoto, T. *Adv. Colloid Interface Sci.* **1987**, *28*, 65.
(3) Sugimoto, T. In *Fine Particles, Synthesis, Characterization, and Mechanisms of Growth*; Sugimoto, T., Ed.; Marcel Dekker: New York, 2000; p 280.
(4) Sugimoto, T.; Sakata, K. *J. Colloid Interface Sci.* **1992**, *152*, 587.
(5) Sugimoto, T.; Itoh, H.; Miyake, H. *J. Colloid Interface Sci.* **1997**, *188*, 101.
(6) Sugimoto, T.; Okada, K.; Itoh, H. *J. Dispersion Sci. Technol.* **1998**, *19*, 143.
(7) LaMer V. K.; Dinegar R. H. *J. Am. Chem. Soc.* **1950**, *72*, 4847.
(8) Berry, C. R. *Photogr. Sci. Eng.* **1976**, *20*, 1.
(9) Wey, J. S.; Strong, R. W. *Photogr. Sci. Eng.* **1977**, *21*, 14.
(10) Wey, J. S.; Strong, R. W. *Photogr. Sci. Eng.* **1977**, *21*, 248.
(11) Strong, R. W.; Wey, J. S. *Photogr. Sci. Eng.* **1979**, *23*, 344.
(12) Leubner, I. H.; Jagannathan, R.; Wey, J. S. *Photogr. Sci. Eng.* **1980**, *24*, 268.
(13) Jagannathan, R.; and Wey, J. S. *Photogr. Sci. Eng.* **1982**, *26*, 61.
(14) Leubner, I. H. *J. Imaging Sci.* **1985**, *29*, 219.
(15) Jagannathan, R.; Wey, J. S. *J. Cryst. Growth* **1985**, *73*, 226.
(16) Jagannathan, R. *J. Imaging Sci.* **1988**, *32*, 100.
(17) Sugimoto, T. *J. Colloid Interface Sci.* **1992**, *150*, 208.
(18) Leubner, I. H. *J. Imaging Sci. Technol.* **1993**, *37*, 510.
(19) Sugimoto, T.; Shiba, F.; Sekiguchi, T.; Itoh, H. *Colloids Surf., A* **2000**, *164*, 183.
(20) Sugimoto, T.; Shiba, F. *Colloids Surf., A* **2000**, *164*, 205.
(21) Sugimoto, T.; Kimijima, K. *J. Phys. Chem. B* **2003**, *107*, 10753.
(22) Kimijima, K.; Sugimoto, T. *J. Phys. Chem. B* **2004**, *108*, 3735.
(23) Shiba, F.; Okawa, Y.; Ohno, T.; Kobayashi, H. *J. Soc. Photogr. Sci. Technol. Jpn.* **2001**, *64*, 77.
(24) Sugimoto, T. *J. Colloid Interface Sci.* **1983**, *93*, 461.
(25) Bush, D. G.; Zuehlke, C. W.; Ballard, A. E. *Anal. Chem.* **1959**, *31*, 1368.
(26) Lin. M. J.; Wey, J. S. U.S. Patent 5,317,521, 1994.
(27) Markocki, W.; Zaleski, A. *Photogr. Sci. Eng.* **1973**, *17*, 289.
(28) Sugimoto, T. *J. Colloid Interface Sci.* **1983**, *91*, 51.
(29) Nakatsugawa, H.; Tani, T. *J. Imaging Sci. Technol.* **2003**, *47*, 78.
(30) Sugimoto, T.; Shiba, F. *J. Phys. Chem. B* **1999**, *103*, 3607.